

Photo-induced absolute negative current in a molecular electronic system.

Alexander Prociuk and Barry D. Dunietz*

*Department of Chemistry
The University of Michigan,
Ann Arbor, Michigan 48109*

Abstract

Negative current in a symmetric 3-state molecular model system can emerge in response to population inversion of electronic excited states induced by photo excitations. The negative current results from the stronger resonance of the populated higher excited band with the source electrode than with the drain, while the lower excited state remains unoccupied. In our treatment, the electronic equations of motion are represented using non-equilibrium Green's functions implementing the Keldysh formalism. Their solution is achieved by using time-dependent perturbation theory.

PACS numbers: 05.60.Gg, 72.40.+w, 73.63.-b, 85.35.Ds, 85.60.Bt, 85.65.+h

Keywords:

The study of electron transport through molecular and nanoscale systems is drawing a large volume of research attention.[1–3] The appeal stems mainly from the technological prospects that nanotechnology is associated with. In addition, the research is driven by the fundamental interest for understanding the complex physics of electron transport processes at the atomic and electronic scale. While the focus of the research has been the steady state, the study of time dependent transport (TD) is becoming of increasing importance. TD studies have revealed interesting quantum effects associated with photo-assisted conductances in mesoscopic systems, such as absolute negative conductance, Coulomb blockade, and Kondo effects driven by alternating-current (AC) fields.[4–7]

The use of AC fields to drive the current has the prospect for reducing the number of contacts required for gating functionality. Electron pumping, where current is driven by TD fields is an example of this research focus.[8–15] In electron pumps direct-current (DC) is generated between unbiased or even negatively biased electrodes. The AC-based gating induces asymmetry of the confined system and in the charge injected across the interfaces.[11, 12, 16, 17] Experimental realizations of directed transport include photo-pumping,[5, 8, 10, 18] Coulomb blockading[19] and adiabatic gating.[11] Theoretical studies provide valuable insight.[12, 13, 17, 20] The use of a monochromatic non-adiabatic driving TD perturbations, which may induce electronic excitations, remains, however, still relatively under explored. This is even more so the case when considering molecular systems, where the need to reduce the number of contacts for the gating functionality becomes of greater importance.[21–23]

We show below that current opposite to an applied constant bias can be induced in molecular junctions by coherent-induced population of a conducting excited electronic state, whereas a related lower excited state remains unoccupied. This pair of states consists of a bonding orbital and a higher anti-bonding state. The negative current will develop if the population inversion between the two conducting states can be sustained. Population inversion is not an easy condition to sustain, however. In a system of two states that are coupled by optical excitations a steady condition develops where both states are equally occupied. Population inversion is achieved in these systems only as a transient via Rabi flopping, which typically requires very intense AC fields. Below we consider the ability of sustaining population inversion using an additional state. Interestingly, this relation of the excited electronic state to negative current is fundamentally analogous to the physics of light

amplification in lasers and optical amplifiers.

This is an important result of general significance. Here, the pumping activity, which is achieved by photo-excitations of molecular model systems, is defined only by the asymmetry induced by a steady and sufficiently weak applied DC bias. We emphasize that while we model molecular junctions similar functionality is expected in coupled quantum dots under the effect of microwave radiation. Our modeling both treats the preparation of the inverted population and demonstrates the resulting negative current. We solve the electronic equations of motion (e.o.m.s) using Keldysh formalism. The equations are expressed by Green functions and their solution is achieved by a TD perturbation theory expansion. Recently, we have implemented several solutions of the electronic equations of motion (the Kadanoff-Baym equations) of model open systems under non-equilibrium conditions [24–26] to analyze TD current and spectroscopy of biased molecular systems. In this report we use the second order dynamical treatment to analyze the effect of photo induced electronic excitations to achieve driven current. We show that at least second order expansions in the TD bias are required to model the driven current.

We start with a bulk-projected form of the electronic e.o.m.s expressed for the case of non-interacting electrons by the lesser GF ($G^<$):

$$\begin{aligned}
i\frac{\partial}{\partial \bar{t}}\Delta\mathbf{G}_{cc}^<(\bar{t},\bar{\omega}) &= [\mathbf{h}_{cc}, \Delta\mathbf{G}_{cc}^<(\bar{t},\bar{\omega})] + \int d\omega'[\mathbf{v}_{cc}(\bar{t},\omega')\mathbf{G}_{cc}^<(\bar{t},\bar{\omega}-\omega') - \mathbf{G}_{cc}^<(\bar{t},\bar{\omega}+\omega')\mathbf{v}_{cc}(\bar{t},\omega')] \\
&+ \int_{-\infty}^{\infty} dt'[\Sigma^{\mathbf{R}}(\bar{t}-t')\Delta\mathbf{G}_{cc}^<(t',\bar{\omega})e^{-i\mathbf{h}_{cc}(\bar{t}-t')} - e^{i\mathbf{h}_{cc}(\bar{t}-t')}\Delta\mathbf{G}_{cc}(t',\bar{\omega})\Sigma^{\mathbf{A}}(t'-\bar{t})],
\end{aligned} \tag{1}$$

where the subscript cc refers to the device central subspace. Here h and S are the Hamiltonian and overlap matrices of the orbital basis functions within the central region. The non-hermitian part of the Hamiltonian due to the coupling to the bulk are denoted as usual by the self-energies Σ . The TD electronic Hamiltonian is $v(t)$, where $\mathbf{v}(\bar{t},\bar{\omega}) = \frac{1}{\pi}e^{-i2\bar{\omega}\bar{t}}\int_{-\infty}^{\infty} dt e^{i(2\bar{\omega})t}\mathbf{v}(t) = \frac{1}{\pi}e^{-i2\bar{\omega}\bar{t}}\tilde{\mathbf{v}}(2\bar{\omega})$. In deriving the e.o.m.s we rewrite[24] the time variables by $\bar{t} \equiv \frac{t_1+t_2}{2}$ and the $\Delta t \equiv t_1-t_2$ and apply a Fourier transform, where $\Delta\omega$ and $\bar{\omega}$ are the inverse frequency-space variables used to express the e.o.m.s in the two-frequency representation. For example using these definitions

$$\mathbf{G}^<(\Delta\omega,\bar{\omega}) \equiv \int_{-\infty}^{\infty} d\bar{t} e^{i\Delta\omega\bar{t}}\mathbf{G}^<(\bar{t},\bar{\omega}). \tag{2}$$

The resulting projected form of the e.o.m. in the full frequency domain is:

$$\begin{aligned} \sum_{k,l} \mathcal{H}_{ijkl}(\Delta\omega) \Delta \mathbf{G}_{CC,kl}^<(\Delta\omega, \bar{\omega}) &= [\mathbf{v}_{CC}(\Delta\omega) \mathbf{G}_{CC}^{0,<}(\bar{\omega} - \Delta\omega/2) - \mathbf{G}_{CC}^{0,<}(\bar{\omega} + \Delta\omega/2) \mathbf{v}_{CC}(\Delta\omega)]_{ij} \\ &+ \frac{1}{\pi} \int d\omega' [\mathbf{v}_{CC}(2\omega') \Delta \mathbf{G}_{CC}^<(\Delta\omega - 2\omega', \bar{\omega} - \omega') - \Delta \mathbf{G}_{CC}^<(\Delta\omega - 2\omega', \bar{\omega} + \omega') \mathbf{v}_{CC}(2\omega')]_{ij}, \end{aligned} \quad (3)$$

where

$$\mathcal{H}_{ijkl}(\Delta\omega) \equiv (\Delta\omega + i\eta - \Delta\epsilon_{ij})\delta_{ik}\delta_{jl} - \Gamma_{ijkl}(\Delta\omega). \quad (4)$$

The projection is achieved by using the electrode self energy expressed in the FD

$$\Gamma_{ijkl}(\Delta\omega) \equiv \int dt e^{i\Delta\omega t} \Gamma_{ijkl}(t) = \Sigma_{ik}^R(\epsilon_j + \Delta\omega)\delta_{lj} - \Sigma_{lj}^A(\epsilon_i - \Delta\omega)\delta_{ik}. \quad (5)$$

These equations can be expanded by substitution to n-th order in the perturbing potential. The solution to these equations are used below to consider the dynamics of a DC-biased system, where a TD perturbation is turned on. For modeling a system at steady state we specialize the same equations to a time-independent perturbation, whose solution is then used to generate the initial state for the dynamical treatment. The final result can be inverse-FT back to the mixed representation to generate Wigner type information that provides important insight on the quantum mechanical effects that determine the time-dependence of the observable (*i. e.* the current operator) as implemented below. Further information on the full derivation of the solution to the e.o.m.s is provided elsewhere. [24–26]

We now solve the e.o.ms as described above for a model molecular system, where electronic excitations are used to control the electronic flow. This current control scheme is based on inducing inverted population within a coupled two state molecular subsystem. An additional lower lying semi bound state localized to the molecule's space is present and is used to sustain the inversion. The three state system as sketched in Figure 1 includes the two molecular electronic states confined between the electrodes, which are coupled strongly to the electrodes via the self energy Σ terms and to each other with the hopping energy β parameter. These couplings produce two broadened conducting channels (broadening is reflected in Fig. 1) with a 2Σ width and whose energy bands are separated by 2β . The additional state is the ground electronic state of the molecular system and is well below the bulk's Fermi energy. It is only slightly broadened through coupling to the conducting states. The ground state coupling is 20 times smaller than the β coupling parameter. This state is therefore strongly

localized to the device region (semi-bound) and is the only occupied state at equilibrium. The total electronic density of states is illustrated in the right panel of Fig. 1. The system is then subjected to a relatively (to the difference between the Fermi energy and the frontier orbitals) weak DC ramping potential of 1V. For this case the DC-induced spectroscopic Stark shifts are negligible.

We consider now the possible electronic state excitations. The ground state is spatially symmetric (bonding). The first and second excited conducting orbitals are bonding and anti-bonding, respectively. Therefore, by the symmetry relations the ground state can be excited only to the second excited state. This transition is still relatively weak in comparison to the first to second excited state transition if made allowed by properly changing the occupations. These spectral features are a consequence of the weak coupling between the ground state and the two unoccupied conducting channels. Nevertheless, this excitation which promotes electronic population from the ground state to the second excited state can be used to sustain population inversion between the two conducting channels. We now emphasize that the small broadening of the ground state replenishes the pumped ground state density and therefore is crucial in enabling the pumping activity.

Next, an AC field is applied across the biased system (V in Fig. 1). The applied AC frequency is tuned to the excitation energy between the ground and the second excited states ($\nu \equiv \omega_0/(2\pi) = 4.1V$). We consider the resulting population transfer induced by the electronic excitation within the coupled system. In Fig. 2 we follow the change of the electronic states' population. In the left panel the time dependence of the occupation of the ground state band is provided. It is shown that the ground state population decreases in response to the excitation. In the right side a color projection of the electronic occupation distribution under the AC bias is provided. As reflected, electronic population is added to the second excited state and is reduced for the ground state following the effects of the applied AC bias. We emphasize that while the occupation of the second electronic excited state increases, the occupation of the first excited state band remains flat at zero. This leads to the condition of inverted population between these two excited states. It is therefore shown that the variations in the population in the device region are indeed due to the ground state losing density for the second excited state. Consequently, the strong bulk-coupling of the excited state results with the transfer of the promoted density to the bulks and to result with the directed current.

We now consider the driven current under the effect of the combined AC laser field and the DC bias as a function of time. The TD current resolved to the different contributions in the TD-PT expansion is provided in Figure 3. In the left panel the real-TD curves of the current are provided. The first order term in the PT expansion is the coherence response to the AC field that features as expected symmetric (about zero) oscillations. The second order term is needed to model the effect of exchange of populations and is associated with negatively directed current. This is also clearly illustrated by the overall current which features bigger negative amplitudes than the positive ones. The generated negative flow is due to the stronger resonance of the higher excited state with the source electrode.

We also analyze the different contributions by studying the spectra of the current operator. In the right panel of Fig. 3 the first order terms are shown to lead to the coherent contribution at the frequency of the excitations. The second order terms are then found at twice that frequency. In addition, the second order terms are shown to lead to zero frequency negative response. The directed current emerges from the population transfer that can be represented only by the second order response to the AC field. Finally, the real-TD curves also include a low pass filtered curve generated from the full TD current. This extracts the non-oscillatory component of the current. The resulting curve clearly features the absolute negative conductance.

The current operator's spectra was used above to resolve the different band contributions to the current. These bands of the current operator can also be directly demonstrated. In the left panel in Fig. 4, the color map projection of the energy resolved current distribution is provided. It includes two major features. The first and more intense feature is a symmetric positive-negative oscillating term, which is due to the interference of the ground and the second excited state. This is the resonant first order response of the current and it involves here two bands with a frequency that is equal to the transition energy. The more dominant first order band is centered at the mid energy of the interfering states. The additional miniband corresponds to the same interferences but is associated with a negative shift below the ground state.[24, 26] The second feature, which is aligned with the higher excited state energy, is negative with superposed oscillations at twice the resonant frequency. This is due to the second order contribution to the current as reflected above in Fig. 3. Electronic population is transferred from the ground state to the second excited state, which is in stronger resonance with the raised band structure of the source lead in response to the

applied bias. This directs the electronic flux oppositely to the applied bias.

Concluding remarks. Transport through open quantum systems follows phase coherence of the charge carriers with the leads. The ability to manipulate these coherences is used to accomplish electron pumping activity in a symmetric model molecular system. The negative current is generated by inducing population inversion between two conducting molecular states that are both strongly coupled to the bulks and to each other. The inversion is due to exciting electron density from an occupied ground state to the second excited state. The ground state is strongly bound to the molecular region and is only indirectly coupled to the electrodes through its weak coupling to the molecular conducting states. The negative flow is then resulting from the stronger resonance of the excited population with the raised band structure of the source electrode. The modeling includes the preparation of the inverted population and the simulation of the resulting negative flow. This is based on solving the electronic equations of motion as expressed by Keldysh formalism using non-equilibrium Green's functions. The calculations employ a time-dependent perturbation theory expansion, where the negative current is associated with the second order term in the expansion.

BDD acknowledges the American Chemical Society Petroleum Research Fund (through Grant 47118-G6) and the University of Michigan for financial support. Acknowledgment is also made to the National Energy Research Scientific Computing Center (NERSC) for awarding computing time.

-
- [1] A. Nitzan and M. A. Ratner, *Science* **300**, 1384 (2003).
 - [2] J. Kushmerick, J. Lazorcik, C. Patterson, R. Shashidhar, D. Seferos, and G. Bazan, *Nano. Lett.* **4**, 639 (2004).
 - [3] F. Chen, J. Hihath, Z. Huang, X. Li, and T. N. J., *Annu. Rev. Phys. Chem.* **58**, 535 (2007).
 - [4] B. J. Keay, S. Zeuner, S. J. Allen, K. D. Maranowski, A. C. Gossard, U. Bhattacharya, and M. J. W. Rodwell, *Phys. Rev. Lett.* **75**, 4102 (1995).
 - [5] T. H. Oosterkamp, L. P. Kouwenhoven, A. E. A. Koolen, N. C. van der Vaart, and C. J. P. M. Harmans, *Phys. Rev. Lett.* **78**, 1536 (1997).
 - [6] P. Nordlander, M. Pustilnik, Y. Meir, N. S. Wingreen, and D. C. Langreth, *Phys. Rev. Lett.*

- 83**, 808 (1999).
- [7] G. Platero and R. Aguado, *Phys. Reports* **395**, 1 (2004).
- [8] L. P. Kouwenhoven, S. Jauhar, J. Orenstein, P. L. McEuen, Y. Nagamune, J. Motohisa, and H. Sakaki, *Phys. Rev. Lett.* **73**, 3443 (1994).
- [9] N. C. van der Vaart, S. F. Godijn, Y. V. Nazarov, C. J. P. M. Harmans, J. E. Mooij, L. W. Molenkamp, and C. T. Foxon, *Phys. Rev. Lett.* **74**, 4702 (1995).
- [10] T. H. Oosterkamp, T. Fujisawa, W. G. van der Wiel, K. Ishibashi, R. V. Hijman, S. Tarucha, and L. P. Kouwenhoven, *Nature* **395**, 873 (1998).
- [11] M. Switkes, C. M. Marcus, K. Campman, and A. C. Gossard, *Science* **283**, 1905 (1999).
- [12] F. Zhou, B. Spivak, and B. Altshuler, *Phys. Rev. Lett.* **82**, 608 (1999).
- [13] S. Kohler, J. Lehmann, and P. Hanggi, *Physics Reports* **406**, 379 (2005).
- [14] M. D. Blumenthal, B. Kaestner, L. Li, S. Giblin, T. J. B. M. Janssen, M. Pepper, D. Anderson, G. Jones, and D. A. Ritchie, *Nat. Phys.* (2007).
- [15] B. Kaestner, V. Kashcheyevs, S. Amakawa, M. D. Blumenthal, L. Li, T. J. B. M. Janssen, G. Hein, K. Pierz, T. Weimann, U. Siegner, et al., *Phys. Rev. B* **77**, 153301 (2008).
- [16] L. Arrachea, C. Naon, and M. Salvay, *Phys. Rev. B* **76**, 165401 (2007).
- [17] G. Stefanucci, S. Kurth, A. Rubio, and E. K. U. Gross, *Phys. Rev. B* **77**, 075339 (2008).
- [18] L. DiCarlo, C. M. Marcus, and J. S. Harris, *Phys. Rev. Lett.* **91**, 246804 (2003).
- [19] L. P. Kouwenhoven, A. T. Johnson, N. C. van der Vaart, C. J. P. M. Harmans, and C. T. Foxon, *Phys. Rev. Lett.* **67**, 1626 (1991).
- [20] C. A. Stafford and N. S. Wingreen, *Phys. Rev. Lett.* **76**, 1916 (1996).
- [21] J. Lehmann, S. Kohler, P. Hänggi, and A. Nitzan, *Phys. Rev. Lett.* **88**, 228305 (2002).
- [22] S. Kohler, S. Camalet, S. M., L. J., G.-L. Ingold, and P. Hanggi, *Chemical Physics* **296**, 243 (2004).
- [23] V. May and O. Kühn, *Phys. Rev. B* **77**, 115440 (2008).
- [24] A. Prociuk and B. D. Dunietz, *Phys. Rev. B* **78**, 165112 (2008).
- [25] A. Prociuk and B. D. Dunietz, *Atomic and Molecular Systems, Dynamics, Spectroscopy, Clusters, and Nanostructures* (Springer, 2009), chap. On the electronic spectra of a molecular bridge under non-equilibrium electric potential conditions.
- [26] A. Prociuk, H. Phillips, and B. D. Dunietz, *Journal of Physics: Conference Series* **Submitted** (2009).

FIG. 1: Schematic diagram of the 3-state system. (left) localized/atomic orbital representation, where the ground state ϵ is weakly coupled (represented by dotted lines) to the conducting channels. The conducting states are coupled strongly to each other and to the leads. (center) Diagonalized molecular orbital representation. (right) Broadened electronic density of states. Only the ground state is below the Fermi energy (FE), which is set to zero.

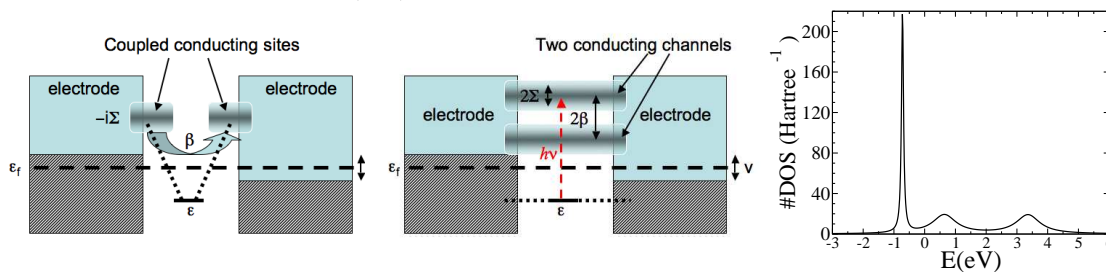


FIG. 2: (left) TD occupation of the ground state. (right) Color map projection of the TD energy distribution of the total density.

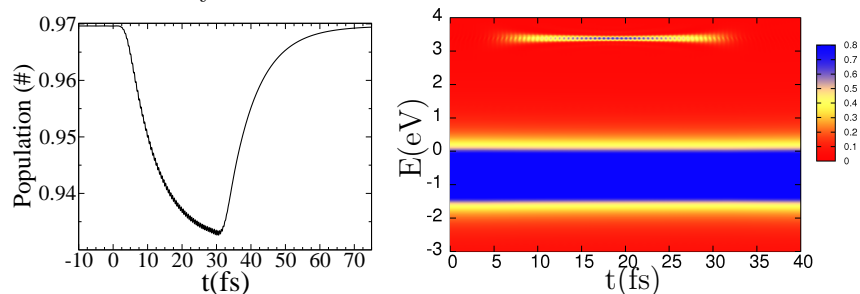


FIG. 3: The current under an applied bias of 1V and an AC field tuned to electronically excite at 4.1V energies. The first and second orders of the TD current (left) in real-time, and (right) its spectral contributions.

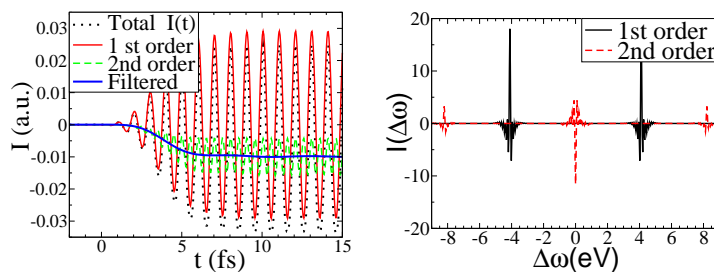


FIG. 4: Color map projection of the TD energy distribution of the (left) current, and (right) the second order corection to the electronic occupations.

